A SHORT HISTORY OF g FACTORS: "ALMOST" 100 YEARS OF g FACTORS

UNA CORTA HISTORIA DE FACTORES g: "CASI" 100 AÑOS DE FACTORES g

Noemie Benczer-Koller, Gerfried J. Kumbartzki

Department of Physics and Astronomy, Rutgers University, New Brunswick, NJ, US

(Recibido: Marzo/2015. Aceptado: Julio/2015)

Abstract

Ever since the discovery of the electron spin and the firm establishment of nuclear physics the study of electromagnetic properties of nuclei has been an important part of nuclear structure research. In particular, the magnitude and sign of the magnetic moment yield a direct measure of the configuration of the nucleons in the nucleus. This presentation is focused on the measurement of magnetic moments of short-lived nuclei with mean lifetimes of fractions to tenths of picoseconds. Many techniques have been developed which make use of the interactions between the nuclear moments and the very high hyperfine magnetic fields generated by the electronic environment. The main elements of the investigations are outlined and a few examples are highlighted. This paper should be read together with the presentation of an in-depth complementary description of relevant reactions, instrumentation, and analysis in Ref. [1].

Keywords: Nuclear g factor, Nuclear magnetic moment, Magnetization.

Noemie Benczer-Koller: nkoller@physics.rutgers.edu

Resumen

El estudio de las propiedades electromagnéticas del núcleo ha sido fundamental en la investigación de la estructura nuclear. En particular, la magnitud y el signo del momento magnético inducen una medida directa de la configuración de los nucleones dentro del núcleo. Este trabajo se focaliza en la medida de los momentos magnéticos de núcleos con tiempos de vida media alrededor de los pico segundos. Muchas técnicas han sido desarrolladas, sacando provecho de la interacción entre los momentos magnéticos y los intensos campos magnéticos hiperfinos generados por el entorno electrónico. Se sugiere leer este artículo, en el que se delinean los principales elementos de estas investigaciones y se subrayan ejemplos relevantes, apoyado en la referencia [1], en donde se detalla la instrumentación, las reacciones relevantes y el análisis de los resultados.

Palabras clave: Factor g nuclear, momento magnético nuclear, Magnetización.

Introduction

In 1922, Stern and Gerlach carried out a fundamental experiment which proved the quantization of angular momentum. Actually Stern was clear on what he wanted to demonstrate, namely "space quantization". A lucid discussion of these early ideas is presented in Ref. [2]. Angular momentum was believed to be generated by the orbital circular motion of electrons. In the old quantum theory the planes of these orbits could only tilt at certain discrete angles with respect to the magnetic field. At that time three positions for this tilt were expected to be possible but Bohr argued that the direction of the plane parallel to the magnetic field would be excluded. Hence only two positions were allowed. Bohr suggested that the magnetic field could split the electron beam into two and only two beams. Spin angular momentum was unknown in 1921 when Stern published the paper "A method using a magnetic field to demonstrate space quantization". Gerlach had interests in molecular beam experiments and was also an expert on

inhomogeneous magnetic fields. Stern needed a strong field gradient to deflect the electron beam according to its space orientation.

The experiment indeed resulted in two beams being detected on photographic plates. Actually the correct interpretation of the experiment could not be offered until four years later, in 1925, when the spin of the electron was postulated [3] as a to understand the observed atomic and molecular spectra.

Classically, the magnetic moment of a current I in a loop of area A and radius r is given by $\mu = \mathrm{IA}$, where $\mathrm{I} = \mathrm{ev}/2\pi\mathrm{r}$, $\mathrm{A} = \pi\mathrm{r}^2$. The magnetic moment is related to the angular momentum $\mathrm{L} = \mathrm{mvr}$ of the system, $\mu = \mathrm{eL}/2\mathrm{m}$.

In quantum mechanical systems, such as atoms or nuclei, the total angular momentum of a particular system is a sum of orbital, l, and spin, s, angular momenta, $j = l + s$. The magnetic moment operator is given by $\overrightarrow{\mu_{op}} = g_l l + g_s s$, where g_l and g_s are dimensionless factors. The magnetic moment can be written in terms of the total angular momentum j and a factor g, $\mu = (\frac{\overrightarrow{\mu_{op}} \cdot \overrightarrow{j}}{j^2})j = g\ j$.

In nuclei, the total angular momentum of a given state is usually denoted by I so that g becomes $g = \frac{\mu/\mu_N}{I/\hbar}$, where μ is written in units of the nuclear magneton, $\mu_N = \mathrm{e}\hbar/2\mathrm{mc}$ and the spin is written in units of $\hbar$. In this expression it is clear that for a single proton or neutron with spin $s = 1/2$ in a state for which $l = 0$, the g factor should be exactly 2. However, the actual single-particle g factor is very different from 2 and, in addition, it is different for protons and neutrons. For protons, g_l =1 and $g_s = 5.587$, while $g_l = 0$ and $g_s =$ –3.826 for neutrons. This particular distinction between the proton and neutron g factors allows for a quantitative differentiation of the contributions of neutrons or protons to the structure of particular states.

In general, for a state wave function ψ denoted by the quantum numbers nlm, the magnetic moment can be calculated for the specific wave function describing the state of interest,

$\mu = < \psi_{nlm} | \overrightarrow{\mu_{op}} | \psi_{nlm} >$.

Moving rapidly forward to modern times and current models, essentially two general approaches have been used too describe

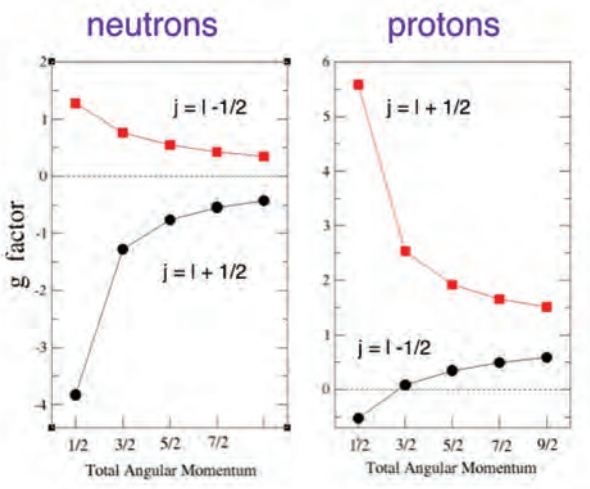

FIGURE 1. *(Color online) Single-particle shell-model predictions for g factors as a function of total angular momentum of a particular nuclear state.*

nuclei: either a single-particle shell-model description [4, 5] of the nucleus or a collective picture [6, 7].

The g factor expected for a single neutron or proton outside closed shells is shown in Fig. 1. Most single-particle g factors are positive except for the g factors of nuclei with single valence neutrons aligned in a $j = l+1/2$ configuration and single $p_{1/2}$ protons. Configuration mixing and meson-exchange corrections need to be considered as well [8, 9].

Calculations based on collective models are more practical in cases where there are large numbers of nucleons beyond shell closures. For collective motions, $g = Z/A$ in first order, with corrections arising from pairing considerations [10] . This value applies to vibrational and deformed rotational nuclei. A simple derivation of this result can be obtained for the case of a simple symmetric rotor. The moment of inertia $\mathcal{J}$ is composed of the moments of inertia of protons $\mathcal{J}_p$ and neutrons $\mathcal{J}_n$. Assuming the protons and neutrons rotate with the same angular velocity the fractional angular momenta for the proton and neutrons become $I_{p,n} = \mathcal{J}_{p,n}/\mathcal{J}$ where I is the total angular momentum. The g factor can be

evaluated from the expression $g = [I_p/I]g_l(p) + [I_n/I]g_l(n) = I_p/I$. If protons and neutrons contribute equally to the rotation, their mass distributions are the same and $\mathcal{J}_p\ /\mathcal{J}_n = Z/N$ and $g = I_p/I = \mathcal{J}_p/\mathcal{J} = \mathcal{J}_p/(\mathcal{J}_p + \mathcal{J}_n) = Z/A$.

However, the observed g factors deviate considerably from the theoretical predictions based on the simple concepts described above, and it is the measurements of these deviations that lead to new theoretical insights.

Measurements

The focus of this presentation is narrowed to the study of short-lived ($\sim$ ps) low-excited states. In order to measure the magnetic moment, the nucleus has to be excited into a state with an aligned total angular momentum, and its decay via gamma rays needs to be observed. An interaction of the state's magnetic moment with a magnetic field H or B, either external or internal (hyperfine interaction), is required. Two types of experiments are carried out most frequently to excite the nuclei of interest. In "normal kinematics", a beam of light nuclei impinges on a heavy target; the opposite occurs in "inverse kinematics" with a beam of heavy nuclei and a light target. The latter approach provides faster, forward moving recoils, and the same target may be used for various beams (isotopes) including radioactive beams for which no stable isotopic target can be prepared for the normal-kinematics condition.

In normal kinematics experiments, Coulomb excitation, charged particle reactions, fusion reactions and the use of fission sources have been used. In inverse kinematics experiments, the main approach has consisted of Coulomb excitation but more recently a reaction in which an α particle is transferred from a ^{12}C target to any beam has also been used. The recoiling ^{8}Be nuclei disintegrate into two α particles that are detected in a detector located at 0° with respect to the beam. These various modes of operation have been described in detail in two review papers and in papers on recent experiments [11–14].

If the reaction produces a nucleus with its spin aligned in a particular direction with respect to the beam, their decay radiation is emitted anisotropically. The g factor can then be determined from the observation of the angular distribution of the decay gamma rays and a knowledge of the magnetic interaction. What is measured is either an energy, $\overrightarrow{\mu} \cdot \overrightarrow{B}$, or a torque, $\overrightarrow{\mu}$ x $\overrightarrow{B}$, leading to a precession angle $\Delta\theta$ of the angular correlation about the direction of the magnetic field B, $\Delta\theta = (g\mu_N/\hbar)B\tau$, where τ is the mean lifetime of the state under study. To determine a precession $\Delta\theta$ in milliradians for states of lifetimes in the microsecond range, a magnetic field of the order of 0.1T, available in laboratory electromagnets, is required. For states with lifetimes shorter than nanoseconds, higher fields became necessary, such as the fields at ions implanted at substitutional sites in ferromagnets. It was observed by Borchers and collaborators [15] that for ions moving initially with appreciable velocity the observed hyperfine interactions corresponded to different fields than those known for nuclei stopped in substitutional sites. Such fields, called "transient" fields, had strengths of about 10 kT and were particularly well-suited for measurements on states with *ps* lifetimes.

There are nearly 100 different types of experimental methods to create a large magnetic field whose interaction with the nuclear magnetic moment results in a measurable precession of the magnetic moment [16]. Some of the commonly used methods involve atomic beam magnetic resonance effects, nuclear magnetic or paramagnetic resonance, nuclear Zeeman (Mössbauer) effect, ion-solid interactions with a static or transient hyperfine field, recoil in vacuum, laser spectroscopy, and trapped ions with laser spectroscopy. In most cases, the ion of interest needs to have been prepared by a nuclear reaction which leaves it in a state with an aligned magnetic moment. In the presence of a magnetic field this moment will precess about the field direction. The measurement of this precession which is proportional to the nuclear magnetic moment and the magnetic field has become the tool of choice. In order to measure magnetic moments of very short-lived states very large magnetic fields are necessary. These have been

found to exist at the nuclei of fast moving, highly stripped, ions traversing polarized magnetic materials, hence their name "transient" magnetic fields [15].

The origin of the observed transient field at the position of the moving ion can be explained qualitatively in the following way. The atoms of the ferromagnetic transition elements, iron and gadolinium, have empty inner shells, 3d in the case of iron, and 4f in the case of gadolinium. If the sample is located in an external external magnetic field it acquires a net electronic spin polarization in a direction opposite to that of the external applied field.

As the moving ion traverses the ferromagnet it could capture polarized electrons from the ferromagnet or, alternately, lose electrons of opposite polarization which go into the empty orbitals of the ferromagnet. In either case the ion ends up with a net ionic polarization in the same direction as that of the ferromagnet. In either case a magnetic interaction between the nuclear magnetic moment and the hyperfine field of its ionic environment ensues causing a net precession of nuclear moment about the axis of polarization.

Subsequent "transient field" calibration experiments were carried out with "thin" ferromagnetic foils, on nuclei whose magnetic moments were known from an unrelated technique. The ions traverse these foils with high velocities and end up stopping in a copper backing where no further magnetic interactions take place. Most often the transit time of the ions through the ferromagnet is shorter than the lifetime of the state under study, and hence uncertainties in the lifetimes do not affect the measurement. The thickness of the foil is chosen so that the ion velocity as it transits through the sample lies within the velocity range that was used for the calibration of the field. These calibration experiments served as the basis for a parametrization of the transient hyperfine field as a function of ion velocity and atomic number of the nucleus [17]. The features of many of the experimental techniques and of the physical processes that lead to a measurable magnetic moment, as well as recently measured g factors are elaborated upon in detail in Ref. [1].

In this presentation, the focus is kept on measurements of the actual magnetization of the iron or gadolinium layers of the targets. In addition, some unexpected g factors are shown to highlight the breadth and potential for new discoveries even for data with only average statistical accuracy.

Measurement of the Magnetization of a Ferromagnetic Foil

The measurements of g factors of particular excited states in nuclei via the transient field technique require a knowledge of the magnitude of the hyperfine magnetic field B_{TF} acting on fast moving nuclei traversing a magnetized ferromagnetic foil. This hyperfine field is directly proportional to the magnetization M of the foil.

The measurement of M is hampered by the fact that the samples are very small (about 1 cm^2 in area and weigh a few milligrams, corresponding to thicknesses of 2 to 10 mg/cm^2). A 60 Hertz ac magnetometer was designed to measure the magnetizations of samples as functions of temperature and applied magnetic fields [18, 19].

The sample whose magnetization is being measured is located at the center of a "pickup"coil. A second identical "bucking" coil, is wound in series with the pickup coil. Both coils are located at the center of a large solenoid producing a uniform oscillating magnetic field of up to 0.1 T at the position of the coils. The bucking coil is needed to separate the small signal induced by the presence of a ferromagnetic sample in the pickup coil from the much larger emf induced by the driving time-varying field. The schematic of the drive, pickup and bucking coils is shown in Fig. 2.

The voltage V induced in the bucking coil is subtracted from that induced in the pickup coil, leaving only the signal due to the magnetization of the sample. More specifically, the integration over the area A of the sample yields

$$V = -N\frac{d}{dt}\int BdA = -N\mu_0\frac{d}{dt}\int(H+M)dA,$$

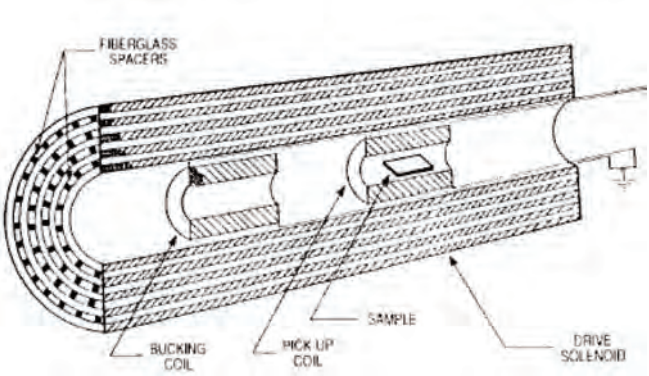

FIGURE 2. *Schematic diagram of the magnetometer driving, pickup and bucking coils. The driving coil is assembled in several individual layers separated by spacers that allow enhanced cooling of the coils by forced air from a fan [18].*

where $\mu_0 = 4\pi$ x 10^{-7} Wb/Am, Am denotes the units Ampere-meters and N is the number of turns of the pickup coil enclosing the sample. The contribution dH/dt from the combined pickup and bucking coils vanishes, hence

$$V = -N\mu_0 \frac{d}{dt} \int M dA$$

If the magnetization is constant throughout the volume of the sample, as is the case when the sample is saturated,

$$V = -N\mu_0 A \frac{dM}{dt} \text{ and } M = -\frac{\int V dt}{N\mu_0 A}$$

The apparatus has a large core that can accommodate a He Displex refrigerator which is able to run the sample at temperatures from 12K to room temperature and is shown in Fig. 3.

Theoretically, the magnetization as a function of temperature follows a Brillouin function which depends on the angular momentum of the atomic state [20]. Thus. if the precession of the magnetic moment in the ferromagnet discussed above is proportional to the magnetization, the precession and magnetization curves should overlap [19]. That situation proved

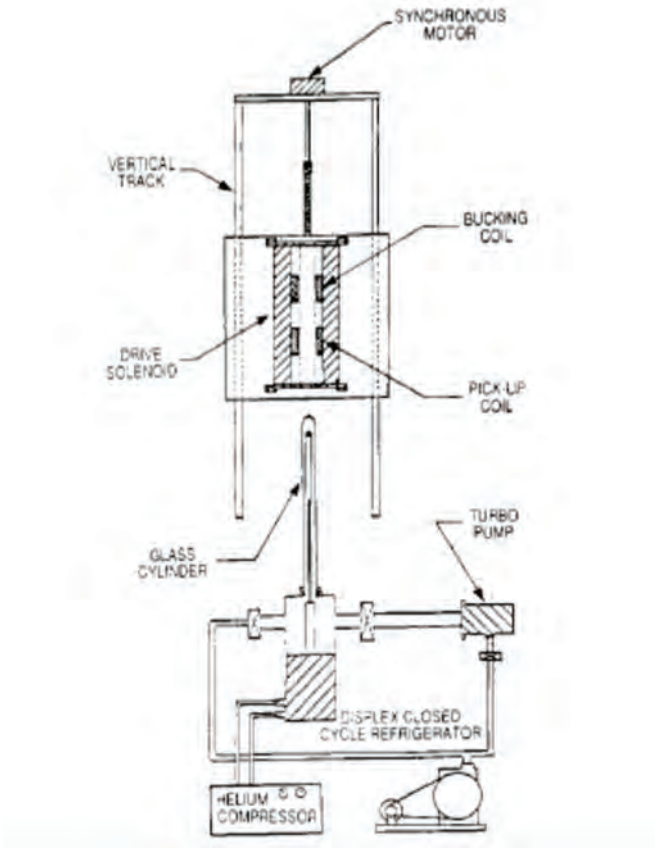

FIGURE 3. *Schematic diagram of the whole magnetometer assembly including coils, cryocooling Displex unit and pumping system. The sample is in a separate glass vacuum enclosure mounted attached to the cryocooler by a sapphire rod. The coils assembly can be moved up and down along a track so that the sample is appropriately positioned at the center of the pickup coil.*

to be the case for the ^{150}Sm 2^+ state (Fig. 4) corroborating the Rutgers formulation of the expected precession [17].

Actually, the magnetization is also strongly dependent on the crystal structure of the foil. The variation of the magnetization of gadolinium as a function of an applied external field, of temperature, and of the direction of the magnetization relative to

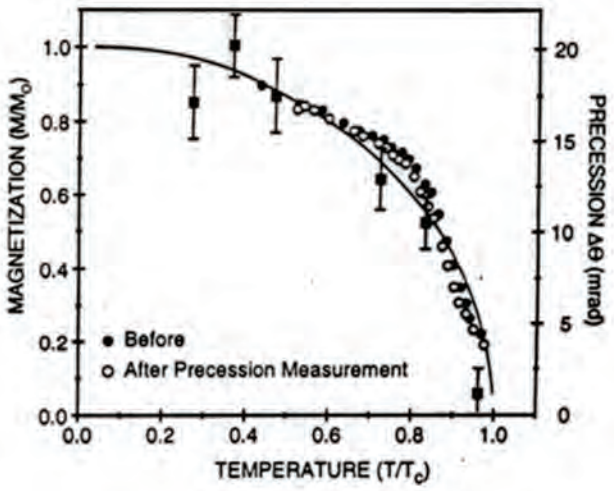

FIGURE 4. *Comparison of the precession measurements (data with error bars) with the magnetization measurements, taken as a function of temperature, both before (filled circles) and after (empty circles) the beam exposure [19].*

the principal axes of the crystal [20, 21] is shown in Fig. 5. This variations are unpredictable because they arise from the process used in the preparation of the foil: rolling or evaporation. Thus, it is imperative that, for each target, the magnetization of the ferromagnetic foil be measured.

In addition, it must be noted that the temperature in the foil at the beam spot position is likely to be higher than the temperature at the rim of the foil where the thermocouple probe is attached, because of energy losses by the beam and recoils in the foil. Hence, two caveats need to be observed in these experiments. The beam intensity has to be kept low to reduce target heating as much as possible. And, the nominal temperature of the foil needs to be at the low end of a relatively flat section of the magnetization curve, so that even some heating of the sample would not result in a reduced magnetization.

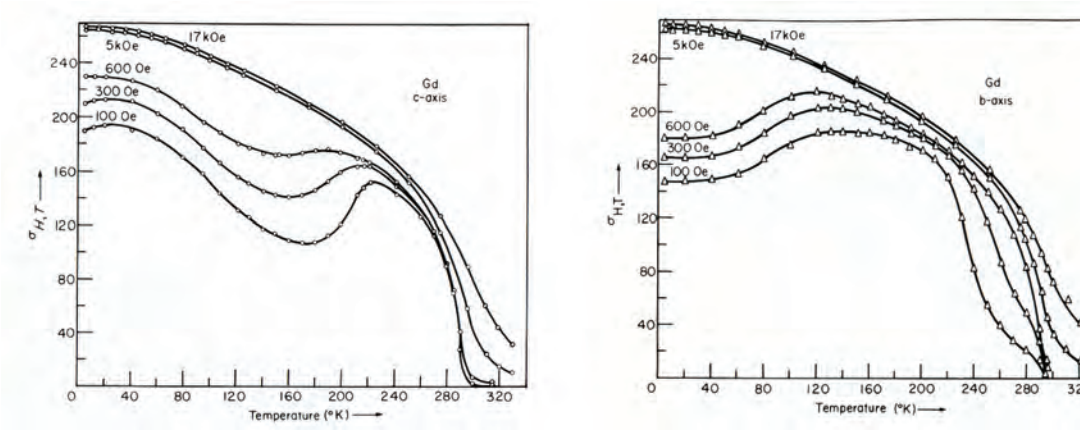

FIGURE 5. *Magnetic moment per gram along the b- and c- axes for a single crystal of gadolinium plotted as a function of temperature (in K) and external applied fields [20, 21].*

Examples of Surprising Results in Light and Heavy Nuclei

This presentation focuses on two sets of data, obtained by Coulomb excitation in inverse kinematics. First, light nuclei, namely the stable semi-magic $_{20}$Ca nuclei, where single-particle effects are modified by collective excitations of protons are discussed. Second, data on the chain of heavy $_{60}$Nd nuclei where collective effects are altered by neutron single-particle contributions, are shown. Examples of measurements on radioactive beams and on nuclei produced in α-capture reactions appear in detail in [1].

In general, 2_1^+ and 4_1^+ states in even-even nuclei have positive g factors. States in even-even nuclei with negative g factors are very rare. The most notable examples of negative g factors have been observed in odd Ca nuclei and in ^{46}Ca, where neutrons occupy the $f_{7/2}$ shell, as well as in ^{18,20}O and in ^{92,94}Zr(2_1^+,4_1^+) isotopes, where neutrons occupy the $d_{5/2}$ orbital. However, there are some outliers. For example, the g factor of the 4_1^+ state in ^{86}Sr is negative, a result attributed to the filling of the $g_{9/2}$ neutron shell. Similarly surprising, the g factors of the 2_1^+ states in ^{42,44}Ca are positive, even

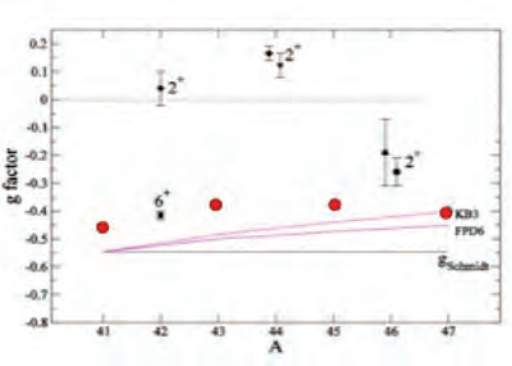

FIGURE 6. *Systematics of $g(2_1^+)$ factors for even, and $g(7/2^-)$ for odd, Ca isotopes. The g factors of $^{44,46}Ca$ have been measured by two different groups [22–24]. The consistency in the results shows the reliability of the transient field technique. The results from two different shell model calculations are also shown together with the Schmidt limit for the g factor for single neutrons in the $f_{7/2}$ shell.*

though the valence neutrons lie in the $f_{7/2}$ orbital for which the g factor should be negative. The experimental data [22–24] and the predictions of shell-model calculations with the two different interactions (KB3 and FPD6) are shown in Fig. 6. The ^{40}Ca isotope has been known for a long time to exhibit important proton particle-hole excitations [25]. These would yield a positive contribution to the g factors of ^{42}Ca and ^{46}Ca. On the other hand ^{48}Ca is supposed to be a better doubly-closed shell than ^{40}Ca, and hence a negative g factor for the 2_1^+ state in ^{46}Ca is observed.

Another interesting example of the effect of configuration mixing as a function of the number of valence neutrons and angular momentum ($I = 2$ to 10) is shown in Fig. 7 for states in the even $_{60}$Nd isotopes ranging from the heaviest, collective, ^{150}Nd to the lightest, ^{142}Nd with a magic number of neutrons, $N = 82$ [26]. The isotope $^{150}_{60}\mathrm{Nd}_{90}$ lies far from magic number in both protons and neutrons and is expected to exhibit a collective, rotational behavior with g factors close to the predicted Z/A limit, independent of spin. However, in spite of larger error bars, the g factor of the 10^+ state is considerably smaller, probably due to significant contributions

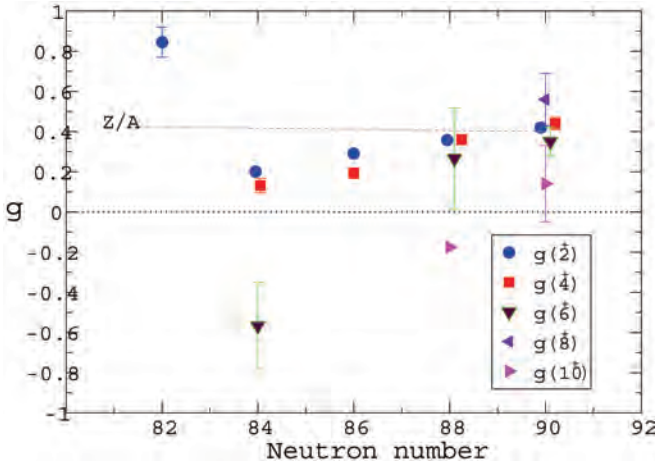

FIGURE 7. (Color online) Systematics of measured $g(I)$ factors for the even Nd isotopes as a function of neutron number and angular momentum I [26].

from neutrons in the $f_{7/2}$ state. Indeed, the adjacent odd isotopes, ^{143,145}Nd have ground state spin $I = 7/2$. This shell effect is even more marked in ^{148}Nd where the low-lying states have smaller g factors than $^{150}_{60}\mathrm{Nd}_{90}$ and the 10^+ state has a definitely negative g factor. As valence neutrons are removed from the Nd nuclei, the g factors are reduced, and decrease systematically as spin increases. The semi-magic $^{142}_{0}\mathrm{Nd}_{82}$ has a very large positive g factor, indicative of proton excitations. However, as many configurations contribute to the wave functions for these Nd nuclei, calculations have proved to be very difficult due to the large valence space, and have not yet been performed.

The systematics of g factors in intermediate mass nuclei, in the region $30 \leq Z \leq 48$, also show interesting features with large variations in the value of the g factors across a particular isotopic chain of nuclei [1]. However, it is obvious that most nuclei exhibit g factors close to the collective value, $g = Z/A$. Recent data have been obtained in the ^{82,90}Sr, ^{88}Zr and ^{100}Pd isotopes [13, 14, 27] and are highlighted in [1]. A snapshot of the data in that region is displayed in Fig. 8. These data highlight the general sparsity of negative g factors, and also show that better statistical accuracy is

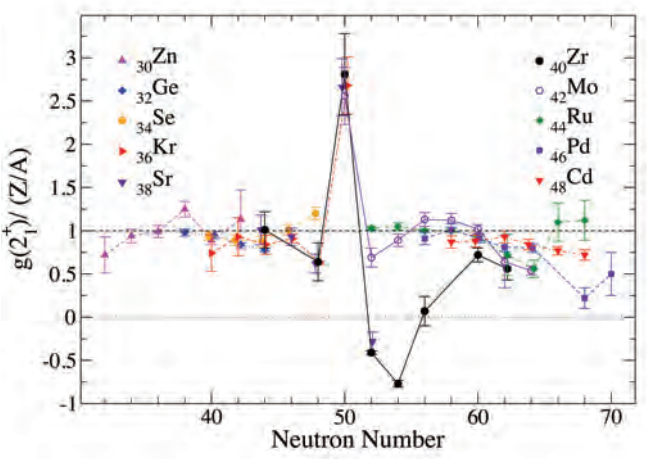

FIGURE 8. *(Color online) Systematics of g factors divided by Z/A for nuclei in the 30 ≤ Z ≤48 range. The lines that connect isotopes are drawn to guide the eye.*

necessary to sharpen the comparison of the data with the theoretical estimates.

Conclusions

The measurements of magnetic moments of nuclear states are a powerful tool in the effort to determine details of the wave function of short-lived states. In the future, measurements need to be extended to the regions beyond stability where an explanation of deviant behavior between theory and experiment is needed to provide missing links in our understanding. The techniques developed for these studies are particularly appropriate for use at the new facilities designed to accelerate nuclei far from stability.

Acknowledgments

This work was supported in part by the US National Science Foundation. The authors are thankful to the sponsors of the 11th Andean School on Nuclear Physics for their travel support to Colombia. The authors acknowledge fruitful discussions with Y. Y. Sharon.

References

[1] G. J. Kumbartzki (2015), Nuclear Magnetic Moments, A Guide to Transient Field Experiments: `http://www.physics.rutgers.edu/~Kum/tfbook.pdf/`.

[2] J. Bernstein (2014), arxiv.org/abs/1007.2435.

[3] G. E. Uhlenbeck and S. Goudsmit, Naturwissenschaften **47**, 953 (1925).

[4] M. G. Mayer, Phys. Rev. **75**, 1969 (1943).

[5] M. G. Mayer, Phys. Rev. **78**, 16 (1950).

[6] A. Bohr and B. Mottelson, Mat. Fys. Medd. Dan. Vid. Selsk. **27**, 1 (1953).

[7] R. F. Casten, Nucl. Phys. **A 443**, 1 (1985).

[8] A. Arima and H. Horie, Prog. Theor. Phys. **11**, 509 (1954).

[9] A. Arima and H. Horie, Prog. Theor. Phys. **12**, 623 (1954).

[10] W. Greiner, Nucl. Phys. **80**, 417 (1966).

[11] N. Benczer-Koller and G. J. Kumbartzki, J. Phys. G: Nucl. Part. Phys. **34**, R321 (2007).

[12] K.-H. Speidel, O. Kenn, and F. Nowacki, Prog. Part. Nucl. Phys. **49**, 91 (2002).

[13] G. J. Kumbartzki, N. Benczer-Koller, S. Burcher, A. Ratkiewicz, S. L. Rice, Y. Y. Sharon, L. Zamick, K.-H. Speidel, D. A. Torres, K. Sieja, et al., Phys. Rev. C **89**, 064305 (2014).

[14] D. A. Torres, G. J. Kumbartzki, Y. Y. Sharon, L. Zamick, B. Manning, N. Benczer-Koller, G. Gürdal, K.-H. Speidel, M. Hjorth-Jensen, P. Maier-Komor, et al., Phys. Rev. C **84**, 044327 (2011).

[15] R. R. Borchers, B. Herskind, J. Bronson, L. Grodzins, R. Kalish, and D. E. Murnick, Phys. Rev. Lett. **20**, 424 (1968).

[16] N. J. Stone, IAEA INDC(NDS)-0594 (2011).

[17] N. K. B. Shu, D. Melnik, J. M. Brennan, W. Semmler, and N. Benczer-Koller, Phys. Rev. C **21**, 1828 (1980).

[18] A. Piqué, J. M. Brennan, R. Darling, R. Tanczyn, D. Ballon, and N. Benczer-Koller, Nucl. Instrum. Methods Phys. Res.

A279, 579 (1989).

[19] N. Benczer-Koller, D. J. Ballon, and A. Pakou, Hyp. Int. **33**, 37 (1983).

[20] R. S. Tebble and D. J. Craik, *Magnetic Materials* (Wiley & Sons, Ltd, London, New York, 1969).

[21] H. E. Nigh, S. Legvold, and F. H. Spedding, Phys. Rev. **132**, 1092 (1964).

[22] M. J. Taylor, N. Benczer-Koller, G. Kumbartzki, T. J. Mertzimekis, S. J. Q. Robinson, Y. Y. Sharon, L. Zamick, A. E. Stuchbery, C. Hutter, C. W. Beausang, et al., Phys. Lett. **B559**, 187 (2003).

[23] M. J. Taylor, N. Benczer-Koller, L. Bernstein, J. Cooper, K. Hiles, D. S. Judson, G. Kumbartzki, P. Maier-Komor, M. A. McMahan, T. J. Mertzimekis, et al., Phys. Lett. B **605**, 265 (2005).

[24] K.-H. Speidel, S. Schielke, O. Kenn, J. Leske, D. Hohn, H. Hodde, J. Gerber, P. Maier-Komor, O. Zell, Y. Y. Sharon, et al., Phys. Rev. C **68**, 061302(R) (2003).

[25] W. J. Gerace and A. M. Green, Nucl. Phys. **A 93**, 110 (1967).

[26] J. Holden, N. Benczer-Koller, G. Jakob, G. Kumbartzki, T. J. Mertzimekis, K.-H. Speidel, C. W. Beausang, R. Krücken, A. Macchiavelli, M. McMahan, et al., Phys. Rev. C **63**, 024315 (2001).

[27] G. J. Kumbartzki, K.-H. Speidel, N. Benczer-Koller, D. A. Torres, Y. Y. Sharon, L. Zamick, S. J. Q. Robinson, P. Maier-Komor, T. Ahn, V. Anagnostatou, et al., Phys. Rev. C **85**, 044322 (2012).